

## Pb(II) ions sequestration from aqueous solutions by canola stalk: isotherms and kinetics studies

Hanie Hashtroudi, Mehdi Khiadani\*, Guangzhi Sun

School of Engineering, Joondalup Campus, Edith Cowan University, 270 Joondalup Drive, Joondalup, Perth, WA 6027, Australia, Tel. +61863045825; Fax: +61863045811; emails: Hhashthro@our.ecu.edu.au (H. Hashtroudi), M.khiadani@ecu.edu.au (M. Khiadani), G.sun@ecu.edu.au (G. Sun)

Received 25 October 2017; Accepted 22 April

---

### ABSTRACT

This study reports on batch adsorption experiments aimed at sequestration of Pb(II) ions from synthetic wastewater at low concentrations onto canola stalk. The surface of the canola stalk was analysed using Fourier transform infrared spectroscopy, scanning electron microscopy, and energy dispersive X-ray spectroscopy systems. The sorption efficiency of the canola stalk for the elimination of lead ions was investigated for a range of pHs, contact times, concentration of lead ions and canola stalk dosages. The experimental data were evaluated applying the Freundlich, Langmuir, Harkins-Jura, Redlich–Peterson and Halsey isotherm equations. The results fitted excellently into the Freundlich and Halsey isotherm models. The Freundlich maximum multilayer sorption capacity was obtained to be 10.923 mg/g. The dynamic mechanism of lead adsorption was investigated over time using pseudo-second-order, pseudo-first-order, Elovich, fractional power and intraparticle diffusion kinetic models. The kinetic study indicated the adsorption data best fitted into the pseudo-second-order equation. The final results demonstrated the effective and fast sorption performance of canola stalk as a low cost and natural adsorbent to treat lead-contaminated wastewater.

*Keywords:* Agricultural waste; Canola stalk; Isotherms; Kinetics; Pb(II) adsorption

---

### 1. Introduction

Heavy metals are toxic contaminants that are mostly distributed in urban stormwater run-off and industrial wastewaters as a result of some mining operations, electronic assembly planting, battery manufacturing and etching operations [1]. Although some of heavy metals are known as important for human life such as Zn, Cu and Fe, some others are recognized as purely toxic heavy metals. Pb(II) is one of the significant harmful heavy metals for human health and the body which is frequently found in industrial wastewater. Drinking lead contaminated water even at low concentrations may cause life-threatening diseases such as cancer, kidney damage, brain damage and liver problems [2]. Therefore, it is necessary to remove lead from aqueous

solutions. Several conventional physical, chemical and biological systems have been used to eliminate Pb(II) ions from contaminated aqueous solutions including membrane filtration, electrolysis, chemical precipitation, magnetic base methods, water filtration and adsorption techniques [3–10]. The cost of some of the cited techniques is prohibitively high, while others cannot remove low Pb(II) ion concentrations efficiently [11,12]. Although adsorption is a reasonable process for removing dissolved lead from contaminated water, the cost of using conventional media (e.g., activated carbon and resin) makes it cost inhibitive for the treatment of large quantities of wastewater [13,14]. It also takes a long time in some cases to achieve adsorption equilibrium [15]. In recent decades, interest in the use of cost-effective adsorbents to reduce the expense of water treatment process has intensified. Attention has been focused on natural agricultural waste materials such as seeds, fruit peel, nut shells, and fruit shells

---

\* Corresponding author.

as low-cost and environmentally friendly adsorbents which are highly efficient and mostly available in large quantities [16–20].

A review of the literature reveals that canola stalk has not been examined as an adsorbent for the elimination of lead ions from contaminated water. This agricultural waste adsorbent has a number of advantages: it is cheap and biodegradable, it has a porousness surface and it is able to subsequent Pb(II) ions from contaminated water quickly and effectively. The main advantage of using natural raw materials as an adsorbent is the usage of chemicals during the water treatment process is minimized. In contrast, chemical and thermal treatments are generally expensive and energy intensive processes and the possibility of releasing unwanted by-products from chemically treated adsorbents into water may create a need for further remediation procedures. Canola stalk has been used in a small number of studies to remove dye and hexavalent chromium from contaminated water [21–24]. Therefore, in this research canola stalk was characterized and its adsorption tendency for the removal of Pb(II) from synthetic lead contaminated water under influence of different experimental factors such as pH, contact time, canola stalk dosage and lead concentration were studied. Various operational conditions were optimized and utilized for isotherm and kinetics modelling.

## 2. Experimental method

### 2.1. Materials and chemicals

The canola stalk for the present study was collected from a local farm in Western Australia. Once collected, the adsorbent was completely washed with deionized water a number of times to remove dust, dirt and lighter soluble contaminants. The washed canola stalk was thoroughly dried in an oven at 100°C for 24 h. This was ground and sieved to attain the desired size of 300 µm maximum. The size of the adsorbent was measured by a Mastersizer (Malvern 3000). Based on the obtained result, more than 90% of the canola stalk particles were under 296 µm.

A serial dilution procedure was used to prepare the desired adsorbate solutions from the high purity stock standard lead (1,000 mg/L) solution. Hydrochloric acid (0.1 mol/L) and the required amount of stock solution were added to the volumetric flask containing deionized water each time. All of the chemicals that were used in this study were obtained from Agilent Technologies Australia and Merck Pty Limited, Australia.

### 2.2. Instruments

In this study the microwave plasma atomic emission spectroscopy (Agilent 4200 MP-AES) was applied to analyse the concentration of lead ions during the experiment. The pH of the solutions was measured by a pH meter (Rowescience WP-90Z). The functional groups of the canola stalk surface were identified using the Fourier transform infrared spectroscopy (FTIR) (PerkinElmer UTAR Spectrum two) within a range of 4,000–400 cm<sup>-1</sup>. Scanning electron microscopy (SEM) (JEOL JSM-6000) was used to determine the characteristics (including roughness) of the adsorbent surface. The chemical

composition of the canola stalk was investigated by energy dispersive X-ray spectroscopy (EDS) (DX200s).

### 2.3. Adsorption batch tests

In this study all of the batch tests were conducted in 100 mL flasks. After adding the necessary amount of canola stalk, the prepared 100 mL solutions were shaken by a temperature-controlled mechanical shaker (RATEK OM11 digital orbital shaking incubator) at 200 rpm. The temperature was kept constant at 23°C during all the batch experiments. The pH of the mixtures was adjusted by adding 0.1 M NaOH and 0.1 M HCl solutions. After stirring the samples for the predetermined desired contact time, the mixtures were filtered out and the aqueous phase of every sample was analysed for its Pb(II) concentration using MP-AES. Different experimental parameters such as initial adsorbent pHs (2–10), contact times (5–120 min), lead concentrations (5–15 mg/L) and dosages (10–30 g/L) were tested to obtain the maximum adsorption capacity of canola stalk. The equilibrium contact time was obtained after testing different predetermined time intervals. The following equations were applied to compute the adsorption capacity of the canola stalk and the percentage of lead ions that were removed:

$$q_e = \frac{(C_i - C_e)V}{D_i} \quad (1)$$

$$\text{Lead removal(\%)} = \left[ \frac{(C_i - C_e)}{C_i} \right] \times 100 \quad (2)$$

where  $q_e$  is the amount of sorption capacity of the canola stalk (mg/g),  $C_i$  and  $C_e$  are the initial lead concentration and equilibrium concentration of Pb(II) (mg/L),  $D_i$  is the initial dosage of canola stalk (g) and  $V$  is the volume of the contaminated solution (L). The mechanism of the adsorption is shown in Fig. 1.

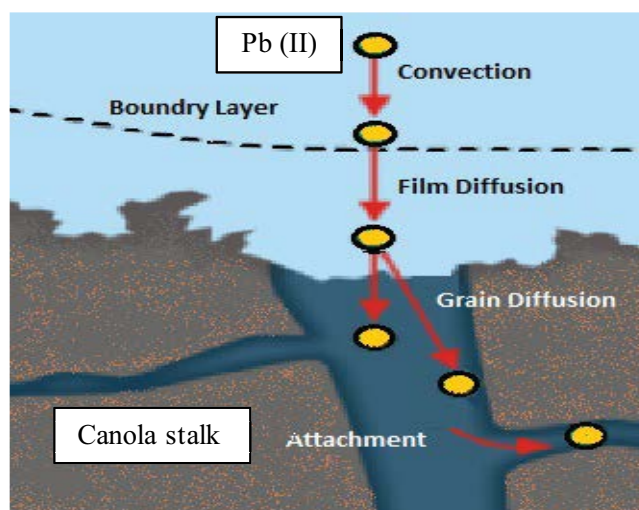


Fig. 1. Scheme of the mechanism of adsorption process.

### 3. Theory of the isotherm and kinetic models

In present study the sorption equilibrium for lead removal from synthetic wastewater using canola stalk was investigated using a number of different isotherm models developed by Langmuir, Harkins-Jura, Freundlich, Redlich–Peterson and Halsey. The Langmuir isotherm is a model developed based on assumptions about the monolayer adsorption process and the homogeneous surface of the adsorbent containing a limited number of active sites [25]. The Langmuir isotherm assumes that all identical adsorption sites have an equal affinity for binding [25]. The Freundlich, Harkins-Jura and Halsey isotherm models are derived by assuming multilayer adsorption onto a heterogeneous adsorbent surface [26,27]. The Redlich–Peterson isotherm is a combination of two isotherm equations (the Langmuir and Freundlich) including three combined elements from these isotherm models [28]. Consequently, the Redlich–Peterson isotherm model could involve multilayer adsorption process [27]. The distribution of active sites and the heterogeneous pore distribution of the adsorbent attest to the possibility of

the multilayer adsorption process in Halsey and Harkins-Jura isotherm models, respectively [29,30]. The adsorption process is strongly influenced by the surface characteristics and chemical compositions of the adsorbent [31]. In this regard, in this study five kinetic models are proposed to evaluate the residence time for lead ion sorption and investigate whether the particle interactions are based on physisorption or chemisorption process. Nonlinear and linear equation forms of all applied isotherm and kinetic models are presented in Table 1. After considering initial and final boundary conditions ( $t = 0 - t$  and  $q_t = 0 - q_t$ ), the nonlinear kinetic equations become linear. All of the constant parameters of the isotherm and kinetic equations can be attained from the slope and intercept of the linear form plots.

### 4. Results and discussion

#### 4.1. Surface characteristics of canola stalk

Different functional groups available on the canola stalk surface were identified by FTIR instrument. The

Table 1  
Nonlinear and linear forms of different isotherm and kinetic models

Isotherm models	Nonlinear form	Linear form	Plot for linear form
Langmuir	$q_e = \frac{b_1 C_e q_1}{1 + b_1 C_e}$	$\frac{C_e}{q_e} = \frac{C_e}{q_1} + \frac{1}{b_1 q_1}$	$\frac{C_e}{q_1}$ vs. $C_e$
Freundlich	$q_e = K_f C_e^{\frac{1}{n_f}}$	$\log(q_e) = \log(K_f) + \frac{1}{n_f} \log(C_e)$	$\log(q_e)$ vs. $\log(C_e)$
Harkins-Jura	$q_e = \left( \frac{A_H}{B_H - \log C_e} \right)^{\frac{1}{2}}$	$\frac{1}{q_e^2} = \left( \frac{B_H}{A_H} \right) - \left( \frac{1}{A_H} \right) \log C_e$	$\frac{1}{q_e^2}$ vs. $\log C_e$
Redlich–Peterson	$q_e = \frac{A_R C_e}{1 + B_R C_e^\beta}$	$\ln \left( A_R \frac{C_e}{q_e} - 1 \right) = \beta \ln C_e + \ln B_R$	$\ln \left( A_R \frac{C_e}{q_e} - 1 \right)$ vs. $\ln C_e$
Halsey	$q_e = \left( \frac{k_H}{\ln(C_e)} \right)^{\frac{1}{n_H}}$	$\ln q_e = \left[ \left( \frac{1}{n_H} \right) \ln k_H \right] - \left( \frac{1}{n_H} \right) \ln C_e$	$\ln q_e$ vs. $\ln C_e$
Kinetic models	Nonlinear form	Linear form	Plot for linear form
Pseudo-first-order	$\frac{dq_t}{dt} = K_f (q_e - q_t)$	$\log(q_e - q_t) = \log(q_e) - \frac{K_f}{2.303} t$	$\log(q_e - q_t)$ vs. time
Pseudo-second-order	$\frac{dq}{dt} = K_s (q_e - q_t)^2$	$\frac{t}{q_t} = \frac{1}{K_s q_e^2} + \frac{1}{q_e} t$	$\frac{t}{q_t}$ vs. time
Intraparticle diffusion		$q_t = K_i t^{\frac{1}{2}} + C_{id}$	$q_t$ vs. $t^{\frac{1}{2}}$
Elovich	$q_t = \frac{1}{\beta} \ln(1 + \alpha \beta t)$	$q_t = \beta \ln(t) + \alpha$	$q_t$ vs. $\ln(t)$
Fractional power	$q_t = \epsilon t^\omega$	$\ln(q_t) = \ln(\epsilon) + \omega \ln(t)$	$\ln(q_t)$ vs. $\ln(t)$

$b_1, q_1$ : Langmuir constants;  $K_f, n_f$ : Freundlich constants;  $A_H, B_H$ : Harkins-Jura constants;  $A_R, B_R, \beta$ : Redlich–Peterson constants;  $k_H, n_H$ : Halsey constants;  $q_t$ : Amount of lead adsorbed by canola stalk at time 't';  $K_f$ : constant value of pseudo-first-order kinetic equation;  $K_s$ : constant value of the pseudo-second-order;  $K_i$  (mg/g min<sup>1/2</sup>) and  $C_{id}$  (mg/g): intraparticle diffusion rate constant values;  $\alpha$  and  $\beta$ : constant values of the Elovich kinetic equation;  $\epsilon$  and  $\omega$ : constant values of the fractional power kinetic equation.

FTIR spectra of the canola stalk before (a) and after (b) the adsorption experiments are shown in Fig. 2. The wavelength was in the range of 4,000–400  $\text{cm}^{-1}$ . Table 2 demonstrates the intramolecular bindings available on the canola stalk surface.

According to the results, canola stalk contains cellulose fibre and lignin owing to the existence of carboxyl, phenol, and hydroxyl groups on its surface [18,34]. Based on the graphs presented in Fig. 2, no major changes can be seen in the FTIR spectra of canola stalk after the experiment.

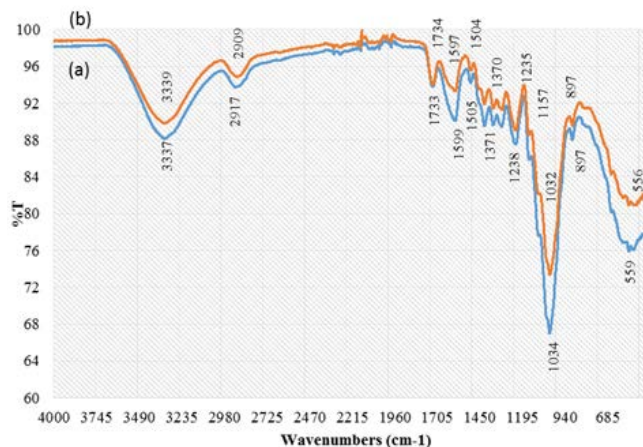


Fig. 2. Canola stalk FTIR spectra before the experiment (a) and after the experiment (b).

Table 2  
FTIR analysis results of the functional groups available on the canola stalk

Wavelength ( $\text{cm}^{-1}$ )	Functional group	References
3,337, 3,339	Overlapping of the different stretching modes of the hydroxyl group	[32,33]
2,917, 2,909	Eminent asymmetric $\text{sp}^3$ -hybridized C–H stretch bond	[18,34]
1,733, 1,734	Aldehyde C=O carboxyl groups	[35]
1,597, 1,599	Aromatic C=C symmetrical stretching	[36]
1,505, 1,504		[37]
1,370, 1,371	C–H bending	[38]
1,238, 1,239	Asymmetric C–O–C stretching bending vibration	[39]
1,157	Nonsymmetric bridge C–O–C vibration	[37]
1,100	C–O valence vibrations of carbohydrate groups	
1,034, 1,032	C–N stretching vibration	[37]
897	Amorphous region	[40]
559, 556	Out-of-plane O–H bending vibrations	[40]

The hydrogen bond distance ( $R_H$ ) is found from the following equations [41]:

$$\Delta v_H = 4,430 \times (2.84 - R_H) \quad (3)$$

$$\Delta v_H = v_M - v_H \quad (4)$$

where  $v_H$  is the OH groups infrared frequency of the canola stalk which were obtained from the FTIR spectra before ( $3,337 \text{ cm}^{-1}$ ) and after ( $3,337 \text{ cm}^{-1}$ ) the experiment and  $v_M$  is the monomeric OH stretching infrared spectrum of the ( $3,600 \text{ cm}^{-1}$ ). The energy of the OH stretching bands is calculated as follows [41,42]:

$$E = \frac{(v_{OH} - v_H)}{Kv_{OH}} \quad (5)$$

where  $K$  is a constant value ( $K = 0.0038 \text{ kJ}$ ), and  $v_{OH}$  is the standard spectrum of the free OH groups, which is taken to be  $3,650 \text{ cm}^{-1}$ . The calculated energy of the OH stretching bond on the surface of canola stalk after the experiment ( $22.37 \text{ kJ}$ ) was found lower than the energy value before the adsorption process ( $22.51 \text{ kJ}$ ). This could be a consequence of adsorbing water during the experiment and the lower quantity of intramolecular OH bonds after the process of adsorption. In contrast, the OH bond distance was found to have a slightly higher value of  $2.781 \text{ \AA}$  after the adsorption of  $\text{Pb(II)}$  ions onto the canola stalk in comparison with the hydrogen bond distance before the experiment  $2.780 \text{ \AA}$ . This may be due to the intramolecular hydrogen bonds between the available phenolic functional groups in lignin and cellulose on the canola stalk surface [38]. A contrary relation between hydrogen bond energy and hydrogen bond distance was observed.

SEM images were captured to compare the surface roughness and morphological aspects of the canola stalk before and after the experiment. Fig. 3 shows the spatial properties of the canola stalk before (a) and after (b) the experiment. As shown in Fig. 3(a), there are numerous holes on the surface of the canola stalk before the experiment. The porosity and roughness of the adsorbent surface enhance the possibility of physical adsorption. The surface of the canola stalk became smoother after the experiment. Fig. 3(c) indicates the result of EDS analysis. Elemental analysis of the canola stalk surface using an EDS system shows that canola stalk contains a high percentage of carbon (85.48%) and 14.52% of oxygen.

#### 4.2. Influence of pH on $\text{Pb}^{+2}$ uptake

Based on the experimental design, a series of batch experiments was performed at different initial pH values (2–10) by adding 10 g/L of canola stalk into 100 mL prepared lead solutions. The experiments were conducted at different lead concentrations (5, 10 and 15 mg/L). All the experiments were conducted at a constant agitation speed of 200 rpm for 120 min and a temperature of  $23^\circ\text{C}$ . The pH of the mixtures was precisely adjusted by adding 0.1 M HCl and 0.1 M NaOH solutions. The pH of the mixture generally has a remarkable influence on the sorption process, so the percentage removal of the lead ions is dependent on the pH value. Due to the

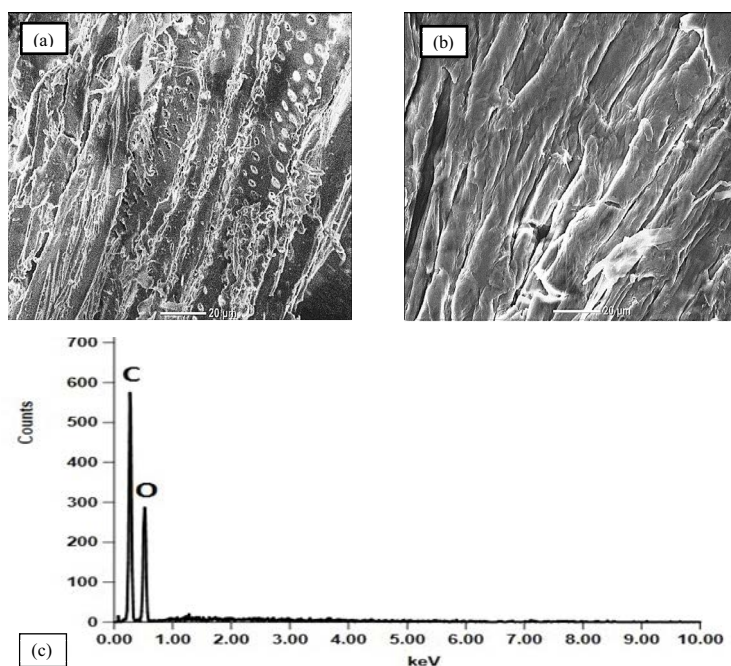


Fig. 3. SEM images of canola stalk before the experiment (a) and after the experiment (b), and EDS spectra of canola stalk (c).

existence of  $H^+$  at lower acidic pHs, the surface of the canola stalk became protonated so the attraction between the positively charged surface and  $Pb^{2+}$  decreases. As shown in Fig. 4(a), by increasing the pH from 2.0 to 4.0, the percentage of  $Pb(II)$  ions removed rose slightly: 96.2%–98% at 5 mg/L lead concentration, 95.8%–97.1% at 10 mg/L lead concentration and 95.4%–96.3% at 15 mg/L lead concentration. After the pH was increased from 4.0 to 6.0 the amount of adsorbed lead ions fell. The uptake of lead ions slightly increased with the rise of the pH from 6.0 to 7.0. For lead concentrations of 5, 10 and 15 mg/L, the percentage removal of  $Pb^{2+}$  was found to be 96.7%, 95.4% and 94.6%, respectively, at pH 7.0. Raising the pH from 8.0 to 10.0 resulted in a small drop of almost 2% for all lead concentrations. This pattern was repeated for different adsorbate concentrations. Adsorption is a complex process affected by different surface characteristics and experimental factors such as microprecipitation, surface charge and the number of anionic binding groups on the adsorbent surface. Thus, the percentage removal of  $Pb^{2+}$  ions was found to be highest at pH 4.0 owing to the efficient exchange of metal cations with anionic groups such as  $-C_6H_5O^-$ ,  $-OH$  and  $-COO^-$  on the canola stalk surface. The electrostatic and van der Waals interactions between the oppositely charged functional groups on the canola stalk surface and  $Pb^{2+}$  ions explain the increased uptake of lead ions at pH 4.0.

#### 4.3. Influence of contact time at different $Pb^{2+}$ concentrations

The influence of contact time was studied by performing a series of experiments with different contact times from 5 to 120 min for various initial metal concentrations (5, 10 and 15 mg/L) at pH 4.0. The temperature and the adsorbent

dosage were kept constant at 23°C and 10 g/L, respectively, during the experiment. The adsorption rate was rapid at the beginning of the adsorption process: after 5 min 95.5%, 94.5% and 93.2% of lead ions were removed at lead concentrations of 5, 10 and 15 mg/L, respectively. The rate of the adsorption became slower in the later stages of the experiment, moving towards saturation at 30 min. The maximum uptakes of  $Pb(II)$  were calculated to be 98%, 97.1% and 96.2% at equilibrium time (30 min) and initial lead concentrations of 5, 10, and 15 mg/L, respectively (Fig. 4(b)). The high extraction efficiency could be due to the interactions between anionic binding groups such as hydroxyl ( $-OH$ ), phenoxide ( $-C_6H_5O^-$ ), and carboxylate ( $-COO^-$ ) and  $Pb^{2+}$  as cations on the canola stalk surface [43]. Moreover due to the great number of active sites on the canola stalk surface, the adsorption rate was quick in the early stage of the process and continued at a slower rate until the saturation of active sites was achieved and equilibrium was reached [43,44].

#### 4.4. Influence of canola stalk dosage on $Pb^{2+}$ uptake

The percentage of  $Pb^{2+}$  removal and the amount of adsorbed lead onto canola stalk per unit at different initial canola stalk dosages (10, 20 and 30 g/L) and initial metal concentrations of 5, 10 and 15 mg/L are shown in Fig. 4(c). All the experiments were conducted at optimized pH 4.0 and equilibrium time of 30 min. The temperature was kept constant during the testing. As shown in Fig. 4(c), the amount of  $Pb^{2+}$  (at concentration of 15 mg/L) adsorbed onto canola stalk was found to be 1.496, 0.496 and 0.297 mg/g per unit at canola stalk dosages of 10, 30 and 50 g/L, respectively. The percentage of lead ion elimination slightly reduced when the metal concentration was increased. This could be the result of the

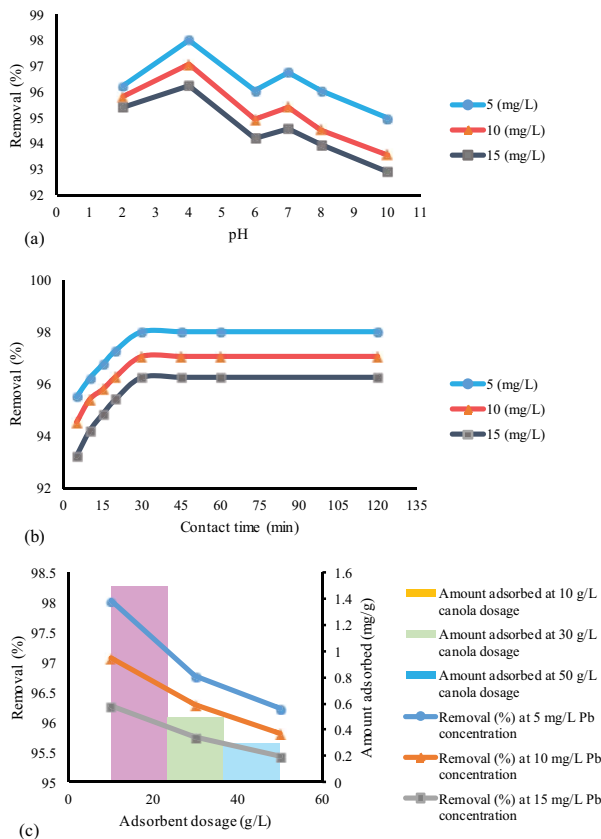


Fig. 4. Influence of pH (a), contact time (b), initial canola stalk dosage (c) on lead removal percentage and sorption capacity of canola stalk at different metal concentrations.

blocking of some adsorption sites due to the agglomeration of  $Pb^{+2}$  ions on the canola stalk surface. In addition, the reduction in the adsorption rate per active site on the canola stalk when the number of particles increased could be the result of a higher number of active sites existing on the canola stalk surface. This would provide more options for the penetration of the  $Pb(II)$  ions on the active sites, which would reduce the adsorption rate.

#### 4.5. Breakthrough and exhaustive capacity

The breakthrough capacity is an important factor in the adsorption process to indicate the efficiency and cost effectiveness of the adsorbent for the removal of the adsorbate [45]. One gram canola stalk was placed into a column (6 mm internal diameter and 22 mm bed height) with glass wool support. 1,000 mL of lead solution with initial concentration of 5 mg/L ( $C_i$ ) was then infiltrate the column at a flow rate of 1 mL/min. The effluent was collected in 150 mL in the beginning and then 50 mL fractions. MP-AES was utilized to determine the residual  $Pb(II)$  concentrations ( $C_e$ ) of each fraction. The breakthrough curve was obtained by plotting  $C_e/C_i$  versus volume of effluent. The exhaustive capacity were found when the  $C_e/C_i = 1$ . Fig. 5 shows that 250 mL of the  $Pb(II)$  solution could pass through the column without detecting lead ions when 1 g of the canola stalk was used.

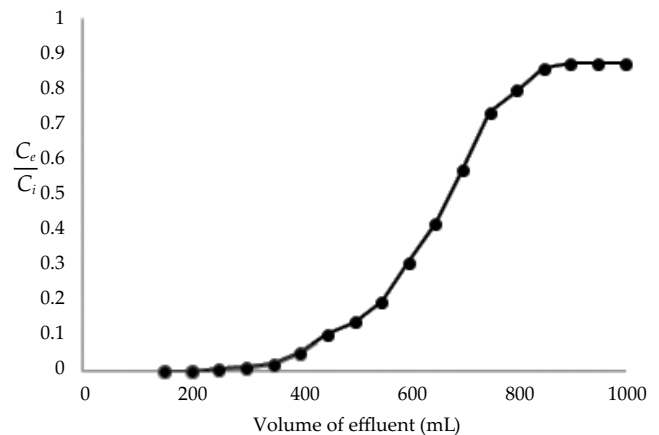


Fig. 5. Breakthrough capacity curve.

The breakthrough and exhaustive capacities were found to be 13.82 and 24.58 (mg/g), respectively.

#### 4.6. Adsorption isotherm models

Based on the obtained experimental data, the relationship between canola stalk dosages and the remaining lead concentrations in the solution can be defined by isotherm equations. The isotherm equations of  $Pb(II)$  ions were used at the previously established optimum pH and contact time. All of the isotherm factors were gained from the intercepts and slope of the linear form plots of Fig. 6. Correlation coefficient values ( $r^2$ ) represent the reliability of isotherm models in regard to the equilibrium data [27]. In this research, the collected adsorption experimental data were evaluated using five different isotherm models. The separation factor of the Langmuir isotherm ( $R_L$ ) can be calculated as follows [46,47]:

$$R_L = \frac{1}{1 + b_L C_i} \quad (6)$$

where  $b_L$  is the Langmuir constant value (L/mg). The  $R_L$  is an indicator that shows the adsorption process is an unfavourable ( $R_L > 1$ ), linear ( $R_L = 1$ ), irreversible ( $R_L = 0$ ) or a favourable process ( $0 < R_L < 1$ ). In this work the values of  $R_L$  were in the range of 0–1, which reflects a desirable adsorption process for the elimination of  $Pb(II)$  using canola stalk.

Table 3 shows the calculated constant parameters of different isotherm equations and correlation coefficient values. According to Table 3, the Harkins-Jura equation is not able to describe the lead adsorption process due to the low correlation coefficient values. The comparison between the Redlich–Peterson and the Langmuir isotherm models indicates that the Redlich–Peterson model predicted the mechanism of adsorption better than the Langmuir equation due to the higher coefficient of correlation. In Table 3 it can be seen that the  $\beta$  values, which are obtained by trial and error, are not close to unity which concludes the isotherms are approaching the Freundlich more than Langmuir isotherm [48].

The highest correlation coefficient values were found for both the Freundlich and Halsey isotherm models. This means that the obtained experimental data of  $Pb(II)$  ions extraction

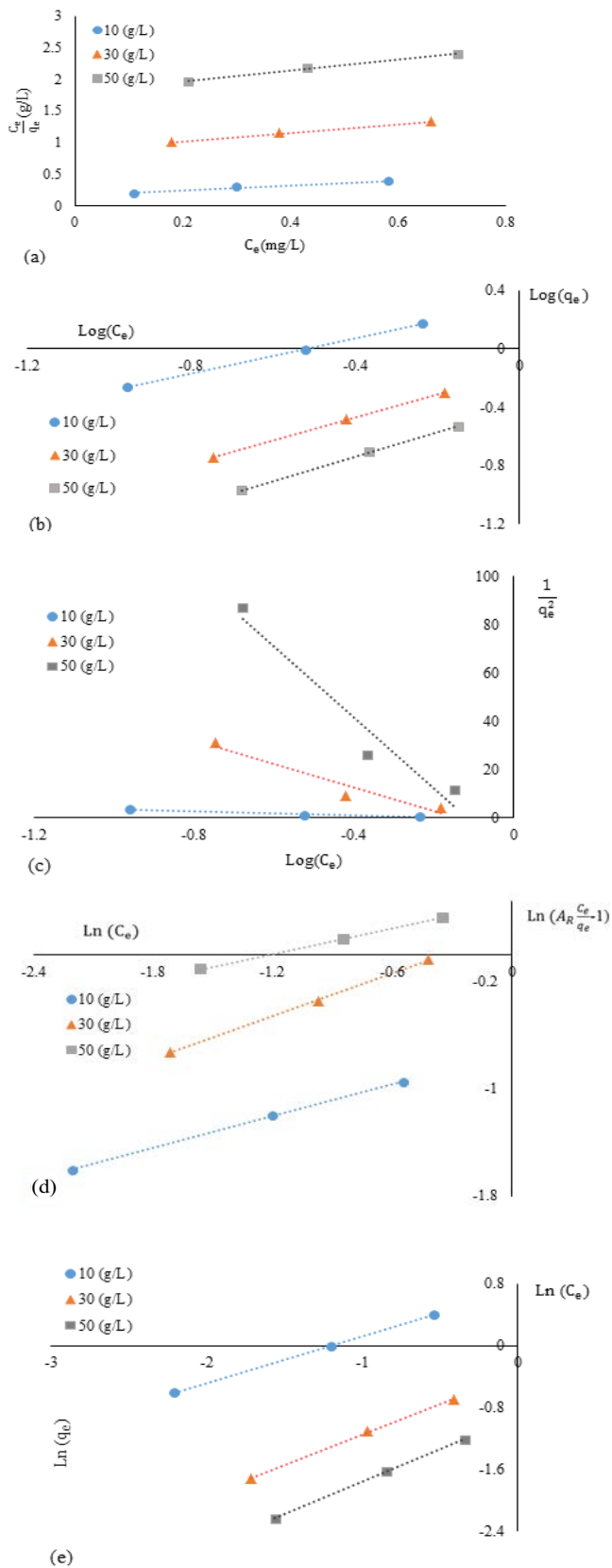


Fig. 6. Langmuir (a), Freundlich (b), Harkins-Jura (c), Redlich-Peterson (d) and Halsey isotherm (e) plots for Pb(II) removal using different dosages of canola stalk.

Table 3

Parameters of the Langmuir, Harkins-Jura, Freundlich, Redlich-Peterson and Halsey isotherm equations for lead adsorption onto canola stalk

Isotherm models and constant parameters	Adsorbent dosage (g/L)		
	10	30	50
Langmuir			
$b_L$ (L/mg)	2.315	0.769	0.481
$Q_1$ (mg/g)	2.567	1.478	1.158
$R_L$	0.027	0.077	0.117
$r^2$	0.9768	0.9968	0.9893
Freundlich			
$1/n_f$	0.606	0.783	0.836
$K_f$	2.073	0.692	0.396
$Q_m$ (mg/g)	10.923	5.935	3.925
$r^2$	0.9999	0.9994	0.9999
Harkins-Jura			
$A_H$	0.242	0.020	0.007
$B_H$	-0.185	-0.145	-0.115
$r^2$	0.9519	0.9364	0.9437
Redlich-Peterson			
$\beta$	0.397	0.535	0.315
$A_R$	5.96	1.48	0.97
$B_R$	0.483	1.203	1.470
$r^2$	0.9997	0.9993	0.9998
Halsey			
$n_H$	1.651	1.277	1.196
$k_H$	3.335	0.625	0.330
$r^2$	0.9999	0.9994	0.9999

onto canola stalk fitted well into the Freundlich and Halsey equations. The Freundlich isotherm is developed based on the assumption that the stronger binding sites are taken first. The affinity for binding reduces while a greater number of sites are occupied [49]. The values of  $1/n_f$  were found to be in the range of 0–1 for the Freundlich isotherm, which indicates a favourable sorption process of Pb(II) ions onto canola stalk. The fact that the achieved experimental data fitted well into the Freundlich and Halsey models may be ascribed to the heterogeneous distribution of active sites and the multilayer sorption process of lead ions onto canola stalk [50,51].

Fig. 7 shows the Freundlich isotherm validation linear plot where,  $q_{exp}$  is the adsorption capacity of lead ions on canola stalk calculated from the experimental results and  $q_f$  is the predicted theoretical adsorption capacity calculated from the Freundlich equation. The coefficient of nondetermination function explains the relationship between the obtained data from the experiments, and the theoretical predicted values from the isotherm equation which can be calculated as follows [27]:

$$\text{Coefficient of nondetermination} = 1 - r^2 \tag{7}$$

The correlation coefficient value of 0.9999 indicates that  $q_{exp}$  and  $q_f$  values are consistent with each other with the coefficient of nondetermination of 0.0001.

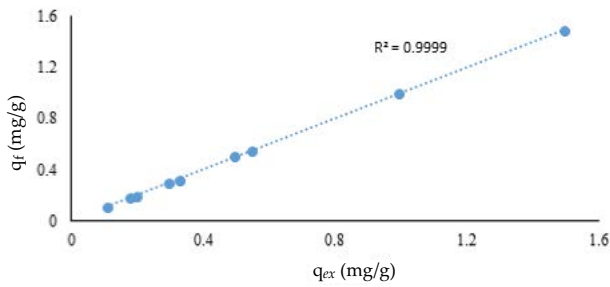


Fig. 7. Freundlich isotherm validation.

Table 4 demonstrates the comparison of the maximum adsorption capacities of lead ions onto various agricultural waste adsorbents. Comparing the results of using canola stalk with other biosorbents for the sequestration of lead ions indicates that canola stalk has a higher adsorption capacity than other adsorbents. According to the obtained high percentage removal of Pb(II) ions (98%) by canola stalk, it can be concluded that canola stalk is highly effective at removing lead from aqueous solutions.

4.7. Adsorption kinetics

The study of kinetics is one of the major characteristics employed in the evaluation of the sorption mechanism. In this work, five kinetic models were applied to the obtained experimental results to study the dynamic mechanism of Pb(II) ion adsorption over time. The pseudo-second-order, pseudo-first-order, Elovich, intraparticle diffusion and fractional power kinetic linear plots are shown in Fig. 8. Table 5 shows the kinetic factors obtained from the linear regression of the plots.

In regard to the correlation coefficient values which are shown in Table 5, the pseudo-first-order, Elovich and fractional power kinetic equations are not suitable for modelling the extraction of Pb(II) onto canola stalk. Although intraparticle diffusion kinetic equation has more potential to estimate the kinetic behaviour of the sorption mechanism, the obtained experimental data fitted into the

Table 4  
Adsorption properties comparison of various adsorbents for Pb(II)

Adsorbent	Maximum sorption capacity (mg/g)	Reference
Canola stalk	10.92	This study
Hazelnut shell	1.78	[52]
Barley straw	4.64	[3]
Coca shell	6.23	[53]
Olive stone	6.39	[54]
Date stem	5.15	[55]
<i>Militia ferruginea</i> plant leaves	3.3	[56]
<i>Gmelina arborea</i> leaves	4.6	[57]

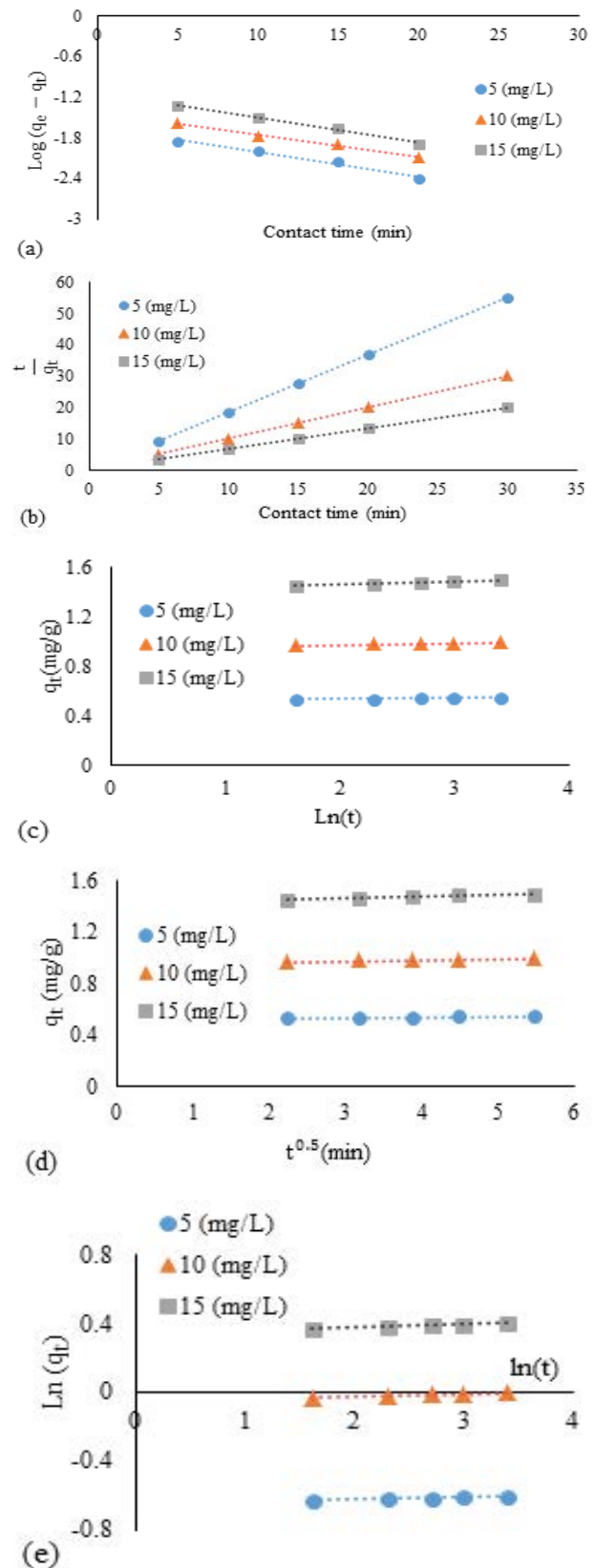


Fig. 8. The pseudo-first-order (a), pseudo-second-order (b), Elovich (c), intraparticle diffusion (d) and fractional power (e) kinetic plots of lead ions adsorbed onto canola stalk.

Table 5

The correlation coefficients and the parameters of the experimental data, pseudo-second-order, pseudo-first-order, fractional power, Elovich and intraparticle diffusion kinetic models

Kinetic models and constant values	Adsorbate concentration (mg/L)		
	5	10	15
Experimental data			
$q_e$	0.546	0.995	1.496
Pseudo-first-order			
$K_f$	0.082	0.076	0.084
$r^2$	0.984	0.989	0.993
Pseudo-second-order			
$K_s$	8.009	4.453	2.447
$q_e$	0.549	1.001	1.507
$r^2$	1	1	1
Elovich			
$\alpha$	0.519	0.946	1.405
$\beta$	0.008	0.014	0.026
$r^2$	0.98	0.983	0.99
Intraparticle diffusion			
$K_i$	0.004	0.008	0.014
$C_i$	0.522	0.952	1.417
$r^2$	0.999	0.995	0.998
Fractional power			
$\varepsilon$	0.519	0.946	1.407
$\omega$	0.014	0.014	0.018
$r^2$	0.98	0.971	0.991

pseudo-second-order kinetic equation best. As seen in Table 5, the highest  $r^2$  values of the pseudo-second-order indicate that the adsorption process of Pb(II) onto canola stalk could be accurately modelled with this kinetic equation. Fitting the obtained experimental data into the pseudo-second-order kinetic equation indicates that the sorption process could be chemisorption involving some valence forces [58]. Moreover, the adsorption rate may be simultaneously controlled by an intraparticle diffusion process. The contribution of the intraparticle diffusion of Pb(II) ions and canola stalk cannot be neglected.

Fig. 9 demonstrates the amount of lead ions adsorbed onto canola stalk at different initial adsorbate concentrations. This parameter ( $q_t$ ) was calculated using the pseudo-first-order, pseudo-second-order, Elovich, intraparticle diffusion and fractional power kinetics equations and was compared with the obtained  $q_t$  values of the experimental data over time.

The sorption capacity of the canola stalk depends on several surface characteristics and experimental factors. The physiochemical nature of the canola stalk including surface area, type and number of anionic functional groups and surface porosity have significant impact on its adsorption ability. At the same time initial pH, canola stalk dosage, Pb(II) concentration and contact time as experimental conditions have an influence on the capacity of the canola stalk to uptake toxic lead ions from synthetic wastewater.

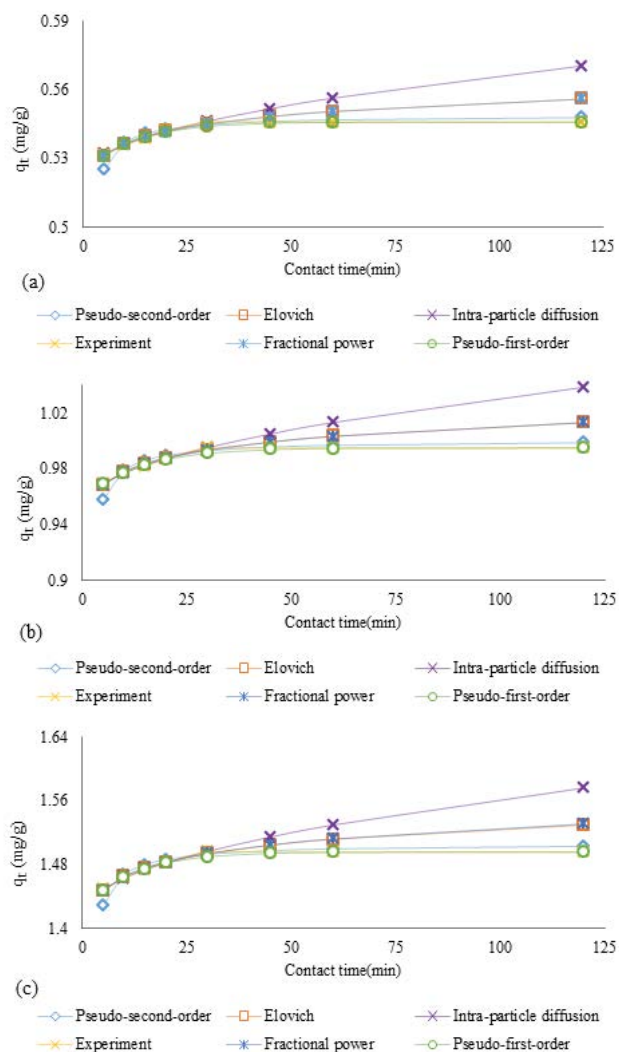


Fig. 9. Amount of Pb(II) ions adsorbed over time at initial adsorbate concentrations of 5 (a), 10 (b) and 15 (c) mg/L using the pseudo-first-order, pseudo-second-order intraparticle diffusion, fractional power, Elovich and experimental data.

## 5. Conclusions

In this study canola stalk was applied as an effective natural agro-waste adsorbent to eliminate toxic Pb(II) ions from synthetic wastewater. The adsorbent was analysed by SEM, EDS and FTIR characterizing systems. The adsorption ability of the canola stalk was studied under different experimental conditions, with variation in initial pHs, contact times, adsorbent dosages and lead concentrations. Based on the presented results, canola stalk demonstrated an excellent adsorption performance with a high extraction capacity of 98% for Pb(II) at pH 4.0 with an equilibrium time of 30 min. The maximum sorption capacity of lead ions onto canola stalk which was computed from the Freundlich isotherm model was found to be 10.923 mg/g. The kinetics study showed that the obtained data from the experiments fitted best into pseudo-second-order model. The mechanism by which canola stalk adsorbs lead might be described as chemisorption via

anionic binding groups followed by some ion exchange and physical interactions. Overall, it can be concluded that canola stalk is an inexpensive, nontoxic and biodegradable adsorbent with ability to quickly and effectively remove Pb(II) ions from the synthetic wastewater.

### Acknowledgements

The authors thank the school of Engineering at Edith Cowan University for funding this project. The authors are thankful to A/Prof Hongqi Sun for his valuable comments. The authors also thank Dr Yong Sun for his technical support.

### References

- [1] K. Kadirvelu, K. Thamaraiselvi, C. Namasivayam, Removal of heavy metals from industrial wastewaters by adsorption onto activated carbon prepared from an agricultural solid waste, *Bioresour. Technol.*, 76 (2001) 63–65.
- [2] A. El-Said, Biosorption of Pb (II) ions from aqueous solutions onto rice husk and its ash, *J. Am. Sci.*, 6 (2010) 143–150.
- [3] E. Pehlivan, T. Altun, S. Parlayıcı, Utilization of barley straws as biosorbents for Cu<sup>2+</sup> and Pb<sup>2+</sup> ions, *J. Hazard. Mater.*, 164 (2009) 982–986.
- [4] J. Song, H. Oh, H. Kong, J. Jang, Polyrhodanine modified anodic aluminum oxide membrane for heavy metal ions removal, *J. Hazard. Mater.*, 187 (2011) 311–317.
- [5] X. Deng, L. Lü, H. Li, F. Luo, The adsorption properties of Pb (II) and Cd (II) on functionalized graphene prepared by electrolysis method, *J. Hazard. Mater.*, 183 (2010) 923–930.
- [6] S.L. Cort, Methods for Removing Heavy Metals from Water Using Chemical Precipitation and Field Separation Methods, Google Patents, 2005.
- [7] Y.-X. Ma, Y.-L. Kou, D. Xing, P.-S. Jin, W.-J. Shao, X. Li, X.-Y. Du, P.-Q. La, Synthesis of magnetic graphene oxide grafted polymaleicamide dendrimer nanohybrids for adsorption of Pb (II) in aqueous solution, *J. Hazard. Mater.*, 340 (2017) 407–416.
- [8] R.J. Gohari, W. Lau, T. Matsuura, E. Halakoo, A. Ismail, Adsorptive removal of Pb (II) from aqueous solution by novel PES/HMO ultrafiltration mixed matrix membrane, *Sep. Purif. Technol.*, 120 (2013) 59–68.
- [9] S. Magni, M. Parolini, C. Soave, F. Marazzi, V. Mezzanotte, A. Binelli, Removal of metallic elements from real wastewater using zebra mussel bio-filtration process, *J. Environ. Chem. Eng.*, 3 (2015) 915–921.
- [10] M. Naushad, Z. AlOthman, M.R. Awual, M.M. Alam, G. Eldesoky, Adsorption kinetics, isotherms, and thermodynamic studies for the adsorption of Pb<sup>2+</sup> and Hg<sup>2+</sup> metal ions from aqueous medium using Ti (IV) iodovanadate cation exchanger, *Ionics*, 21 (2015) 2237–2245.
- [11] B. Volesky, Z. Holan, Biosorption of heavy metals, *Biotechnol. Progr.*, 11 (1995) 235–250.
- [12] S. Babel, T.A. Kurniawan, Low-cost adsorbents for heavy metals uptake from contaminated water: a review, *J. Hazard. Mater.*, 97 (2003) 219–243.
- [13] A. Demirbas, Heavy metal adsorption onto agro-based waste materials: a review, *J. Hazard. Mater.*, 157 (2008) 220–229.
- [14] L. Cutillas-Barreiro, R. Paradelo, A. Igrexas-Soto, A. Núñez-Delgado, M.J. Fernández-Sanjurjo, E. Álvarez-Rodríguez, G. Garrote, J.C. Nóvoa-Muñoz, M. Arias-Estévez, Valorization of biosorbent obtained from a forestry waste: competitive adsorption, desorption and transport of Cd, Cu, Ni, Pb and Zn, *Ecotoxicol. Environ. Saf.*, 131 (2016) 118–126.
- [15] I. Czinkota, R. Földényi, Z. Lengyel, A. Marton, Adsorption of propisochlor on soils and soil components equation for multi-step isotherms, *Chemosphere*, 48 (2002) 725–731.
- [16] M.M. Ibrahim, W.W. Ngah, M. Norliyana, W.W. Daud, Y. Rafatullah, O. Sulaiman, R. Hashim, A novel agricultural waste adsorbent for the removal of lead (II) ions from aqueous solutions, *J. Hazard. Mater.*, 182 (2010) 377–385.
- [17] U.A. Gilbert, I.U. Emmanuel, A.A. Adebajo, G.A. Olalere, Biosorptive removal of Pb<sup>2+</sup> and Cd<sup>2+</sup> onto novel biosorbent: defatted *Carica papaya* seeds, *Biomass Bioenergy*, 35 (2011) 2517–2525.
- [18] R. Mallampati, L. Xuanjun, A. Adin, S. Valiyaveetil, Fruit peels as efficient renewable adsorbents for removal of dissolved heavy metals and dyes from water, *ACS Sustainable Chem. Eng.*, 3 (2015) 1117–1124.
- [19] Ş. Taşar, F. Kaya, A. Özer, Biosorption of lead(II) ions from aqueous solution by peanut shells: equilibrium, thermodynamic and kinetic studies, *J. Environ. Chem. Eng.*, 2 (2014) 1018–1026.
- [20] R. Zein, R. Suhaili, F. Earnestly, E. Munaf, Removal of Pb (II), Cd (II) and Co (II) from aqueous solution using *Garcinia mangostana* L. fruit shell, *J. Hazard. Mater.*, 181 (2010) 52–56.
- [21] Y. Hamzeh, E. Azadeh, S. Izadyar, M. Layeghi, A. Abyaz, Y. Asadollahi, Utilization of canola stalks in the decolorization of reactive dye contaminated water, *JFWP*, 63 (2011) 409–419.
- [22] Y. Hamzeh, E. Azadeh, S. Izadyar, I. Karaj, Removal of reactive Remazol Black B from contaminated water by lignocellulosic waste of canola stalks, *J. Color Sci. Technol.*, 5 (2011) 77–85.
- [23] D. Balarak, J. Jaafari, G. Hassani, Y. Mahdavi, I. Tyagi, S. Agarwal, V.K. Gupta, The use of low-cost adsorbent (Canola residues) for the adsorption of methylene blue from aqueous solution: isotherm, kinetic and thermodynamic studies, *Colloids Interface Sci. Commun.*, 7 (2015) 16–19.
- [24] A. Amouei, M.-H. Ehrampoush, M.-T. Ghaneian, F. Asgharzadeh, A. Mousapour, H. Parsian, Removing cadmium from aqueous solutions by the Canola residuals, *J. Mazand Univ. Med. Sci.*, 23 (2014) 153–164.
- [25] I. Langmuir, The constitution and fundamental properties of solids and liquids. Part I. Solids, *J. Am. Chem. Soc.*, 38 (1916) 2221–2295.
- [26] H. Freundlich, Über die adsorption in lösungen, *Z. Phys. Chem.*, 57 (1907) 385–470.
- [27] N. Ayawei, A.N. Ebelegi, D. Wankasi, Modelling and interpretation of adsorption isotherms, *J. Chem.*, 2017 (2017) 11 pages.
- [28] K. Foo, B.H. Hameed, Insights into the modeling of adsorption isotherm systems, *Chem. Eng. J.*, 156 (2010) 2–10.
- [29] N.K. Amin, Removal of direct blue-106 dye from aqueous solution using new activated carbons developed from pomegranate peel: adsorption equilibrium and kinetics, *J. Hazard. Mater.*, 165 (2009) 52–62.
- [30] C.A. Başar, Applicability of the various adsorption models of three dyes adsorption onto activated carbon prepared waste apricot, *J. Hazard. Mater.*, 135 (2006) 232–241.
- [31] T.A. Saleh, G.I. Danmaliki, Influence of acidic and basic treatments of activated carbon derived from waste rubber tires on adsorptive desulfurization of thiophenes, *J. Tai Inst. Chem. Eng.*, 60 (2016) 460–468.
- [32] M.-C. Popescu, C.-M. Popescu, G. Lisa, Y. Sakata, Evaluation of morphological and chemical aspects of different wood species by spectroscopy and thermal methods, *J. Mol. Struct.*, 988 (2011) 65–72.
- [33] T. Kondo, The assignment of IR absorption bands due to free hydroxyl groups in cellulose, *Cellulose*, 4 (1997) 281–292.
- [34] D.H.K. Reddy, K. Seshiah, A. Reddy, M.M. Rao, M. Wang, Biosorption of Pb<sup>2+</sup> from aqueous solutions by *Moringa oleifera* bark: equilibrium and kinetic studies, *J. Hazard. Mater.*, 174 (2010) 831–838.
- [35] R. Han, L. Zhang, C. Song, M. Zhang, H. Zhu, L. Zhang, Characterization of modified wheat straw, kinetic and equilibrium study about copper ion and methylene blue adsorption in batch mode, *Carbohydr. Polym.*, 79 (2010) 1140–1149.
- [36] M. Poletto, A.J. Zattera, R. Santana, Structural differences between wood species: evidence from chemical composition, FTIR spectroscopy, and thermogravimetric analysis, *J. Appl. Poly. Sci.*, 126 (2012) E337–E344.
- [37] M. Fan, D. Dai, B. Huang, Fourier transform infrared spectroscopy for natural fibres, *Fourier Transform-Materials Analysis*, InTech, 2012.
- [38] C.-M. Popescu, M.-C. Popescu, G. Singurel, C. Vasile, D.S. Argyropoulos, S. Willfor, Spectral characterization of eucalyptus wood, *Appl. Spectrosc.*, 61 (2007) 1168–1177.

- [39] M. Rafatullah, O. Sulaiman, R. Hashim, A. Ahmad, Adsorption of copper (II), chromium (III), nickel (II) and lead (II) ions from aqueous solutions by meranti sawdust, *J. Hazard. Mater.*, 170 (2009) 969–977.
- [40] J. Coates, Interpretation of Infrared Spectra, A Practical Approach, *Enc Anal Chem*, 12 (2000) 10815–10837.
- [41] G.C. Pimentel, C.H. Sederholm, Correlation of infrared stretching frequencies and hydrogen bond distances in crystals, *J. Chem. Phys.*, 24 (1956) 639–641.
- [42] H. Struszczyk, Modification of lignins. III. Reaction of lignosulfonates with chlorophosphazenes, *J. Macromol. Sci. Chem.*, 23 (1986) 973–992.
- [43] M. Haris, K. Sathasivam, The removal of methyl red from aqueous solutions using modified banana trunk fibers, *Arch. Appl. Sci. Res.*, 2 (2010) 209–216.
- [44] A. Babarinde, G.O. Onyiaocha, Equilibrium sorption of divalent metal ions onto groundnut (*Arachis hypogaea*) shell: kinetics, isotherm and thermodynamics, *Chem. Int.*, 2 (2016) 37–46.
- [45] M. Ghasemi, M. Naushad, N. Ghasemi, Y. Khosravi-Fard, A novel agricultural waste based adsorbent for the removal of Pb (II) from aqueous solution: kinetics, equilibrium and thermodynamic studies, *J. Ind. Eng. Chem.*, 20 (2014) 454–461.
- [46] M. Naushad, Z. AlOthman, H. Javadian, Removal of Pb (II) from aqueous solution using ethylene diamine tetra acetic acid-Zr (IV) iodate composite cation exchanger: kinetics, isotherms and thermodynamic studies, *J. Ind. Eng. Chem.*, 25 (2015) 35–41.
- [47] M. Naushad, T. Ahamad, B.M. Al-Maswari, A.A. Alqadami, S.M. Alshehri, Nickel ferrite bearing nitrogen-doped mesoporous carbon as efficient adsorbent for the removal of highly toxic metal ion from aqueous medium, *Chem. Eng. J.*, 330 (2017) 1351–1360.
- [48] F.-C. Wu, B.-L. Liu, K.-T. Wu, R.-L. Tseng, A new linear form analysis of Redlich–Peterson isotherm equation for the adsorptions of dyes, *Chem. Eng. J.*, 162 (2010) 21–27.
- [49] R. Negi, G. Satpathy, Y.K. Tyagi, R.K. Gupta, Biosorption of heavy metals by utilising onion and garlic wastes, *Int. J. Environ. Pollut.*, 49 (2012) 179–196.
- [50] T.A. Khan, M. Nazir, E.A. Khan, Adsorptive removal of rhodamine B from textile wastewater using water chestnut (*Trapa natans* L.) peel: adsorption dynamics and kinetic studies, *Toxicol. Environ. Chem.*, 95 (2013) 919–931.
- [51] C. Song, S. Wu, M. Cheng, P. Tao, M. Shao, G. Gao, Adsorption studies of coconut shell carbons prepared by KOH activation for removal of lead (II) from aqueous solutions, *Sustainability*, 6 (2013) 86–98.
- [52] G. Cimino, A. Passerini, G. Toscano, Removal of toxic cations and Cr (VI) from aqueous solution by hazelnut shell, *Water Res.*, 34 (2000) 2955–2962.
- [53] N. Meunier, J. Laroulandie, J. Blais, R. Tyagi, Cocoa shells for heavy metal removal from acidic solutions, *Bioresour. Technol.*, 90 (2003) 255–263.
- [54] G. Blázquez, M. Calero, F. Hernáinz, G. Tenorio, M. Martín-Lara, Equilibrium biosorption of lead (II) from aqueous solutions by solid waste from olive-oil production, *Chem. Eng. J.*, 160 (2010) 615–622.
- [55] H. Yazid, R. Maachi, Biosorption of lead (II) ions from aqueous solutions by biological activated dates stems, *J. Environ. Sci. Technol.*, 1 (2008) 201–213.
- [56] A.A. Mengistie, T.S. Rao, A.P. Rao, M. Singanan, Removal of lead (II) ions from aqueous solutions using activated carbon from *Militia ferruginea* plant leaves, *Bull. Chem. Soc. Ethiop.*, 22 (2008) 349–360.
- [57] J.O. Tijani, M. Musah, I. Blessing, Sorption of lead (II) and copper (II) ions from aqueous solution by acid modified and unmodified *Gmelina arborea* (Verbenaceae) leaves, *J. Emerg. Trends Eng. Appl. Sci.*, 2 (2011) 734–740.
- [58] W. Song, B. Gao, T. Zhang, X. Xu, X. Huang, H. Yu, Q. Yue, High-capacity adsorption of dissolved hexavalent chromium using amine-functionalized magnetic corn stalk composites, *Bioresour. Technol.*, 190 (2015) 550–557.